

DETC2011-48533

**SERVO-CONSTRAINT BASED COMPUTED TORQUE CONTROL OF
UNDERACTUATED MECHANICAL SYSTEMS**

László L. Kovács*
József Kövecses

Centre for Intelligent Machines
Department of Mechanical Engineering
McGill University, Montréal, Québec, Canada
Email: kovacs@cim.mcgill.ca, jozsef.kovecses@mcgill.ca

Ambrus Zelei
László Bencsik
Gábor Stépan

Department of Applied Mechanics
Budapest University of Technology and Economics
Budapest, Hungary
Email: {zelei,bencsik,stepan}@mm.bme.hu

ABSTRACT

This paper aims to generalize the computed torque control method for underactuated systems which are modeled by a non-minimum set of generalized coordinates subjected to geometric constraints. The control task of the underactuated robot is defined in the form of servo constraint equations that have the same number as the number of independent control inputs. A PD controller is synthesized based on projecting the equations of motion into the nullspace of the distribution matrix of the actuator forces/torques. The results are demonstrated by numerical simulation and experiments conducted on a two degrees-of-freedom device.

INTRODUCTION

Computed torque control of robotic systems is a control method that is often applied in various applications which require high accuracy [1]. By employing the concept of underactuation it is also possible to build agile and energy efficient devices by exploiting the natural dynamics of these systems. Their control design is, however, challenging due to the fact that the inverse dynamics problem cannot be solved directly, since the number of actuators is less than the number of degrees-of-freedom of the system. In addition, when the nonlinear dynamics of the controlled mechanical system has to be considered, modeling and/or computational difficulties may arise.

In case of constrained dynamical systems, such as closed-loop manipulators or robots contacting their environments, the kinematic constraint conditions have to be considered explicitly during dynamics modeling and analysis. These systems are often described by a non-minimum set of generalized coordinates subjected to constraints that provide an efficient formalism to generate the equations of motion. These equations, however, form a system of differential-algebraic equations (DAE).

Control techniques, e.g., partial feedback linearization (PFL) [2] and the computed desired computed torque control method (CDCTCM) [3], are available only for underactuated systems that are modeled by a minimum set of generalized coordinates. These models can either directly be derived by using a minimum set of generalized coordinates or they can be obtained from models having non-minimum set of generalized coordinates. The transformation between these two representations is always possible but it requires the use of a mixed set of generalized coordinates and the corresponding calculations can be time consuming.

In some cases the advantage of using the non-minimum set of descriptor coordinates is to have a model which can effectively be simulated. For example, using natural coordinates [4] the mass matrix of the modeled dynamical system is constant and the constraint Jacobian is often linear function of these coordinates that enable the real time solution of the equation of motion of complex mechanical systems.

*Address all correspondence to this author.

This work presents a possible generalization of the computed torque control method applied for underactuated systems which are modeled by using a non-minimum set of generalized coordinates. An important element of the presented approach is the use of the concept of servo-constraints specifying the motion of the constrained system as function of the generalized coordinates and time [5]. The proposed strategy is based on the projection of the equations of motion into the nullspace of the distribution matrix of the actuator forces/torques, and on stabilizing the servo constraints by a PD controller. The applicability of the investigated computed torque strategy is demonstrated by simulations and by experiments conducted on a two degrees-of-freedom (DoF) robot with one actuator.

GENERALIZED COMPUTED TORQUE CONTROL

The control methods of PFL and CDCTCM are especially devoted to control underactuated systems described by minimum sets of generalized coordinates [2, 3]. The PFL can be used to feedback linearize the dynamics corresponding to the active DoFs (collocated case), and in case of strong inertial coupling, the dynamics corresponding to the passive DoFs of a system (non-collocated case), respectively. Within the categories of passive and active DoFs, reference [3] introduces controlled and uncontrolled DoFs. The trajectories of the uncontrolled coordinates are calculated on-line which makes the error feedback for all the DoFs possible. The online calculation of these coordinates requires the solution of the equation of motion projected into the space of uncontrolled motion. This projection is possible by using the nullspace of the distribution (coefficient) matrix of the input force/torque vector.

Following the same idea reference [6] presents a computed torque based solution for the position control of a suspended service robot modeled by a non-minimum set of generalized coordinates. In this paper, the desired values of the uncontrolled coordinates and the computed forces/torques were determined via the direct solution of the differential algebraic equations of motion by applying backward Euler discretization and the Newton-Raphson method to solve the resulting nonlinear set of algebraic equations. By introducing the concept of servo constraints [5], here, a computationally more effective computed torque control strategy is proposed.

It is assumed that the dynamics of the underactuated system is modeled by using a non-minimum set of generalized coordinates. Then the equation of motion of the system has the general form

$$\mathbf{M}(\mathbf{q})\ddot{\mathbf{q}} + \mathbf{c}(\mathbf{q}, \dot{\mathbf{q}}) + \Phi_{\mathbf{q}}^T(\mathbf{q})\boldsymbol{\lambda} = \mathbf{Q}_g(\mathbf{q}) + \mathbf{H}(\mathbf{q})\mathbf{u} \quad (1)$$

$$\boldsymbol{\phi}(\mathbf{q}) = \mathbf{0} \quad (2)$$

where $\mathbf{M}(\mathbf{q}) \in \mathbb{R}^{n \times n}$ is the mass matrix of the system,

$\mathbf{C}(\mathbf{q}, \dot{\mathbf{q}}) \in \mathbb{R}^n$ is the vector that contains the Coriolis, centrifugal and damping terms and $\Phi_{\mathbf{q}}(\mathbf{q}) = \partial\boldsymbol{\phi}(\mathbf{q})/\partial\mathbf{q} \in \mathbb{R}^{m \times n}$ is the Jacobian associated with the geometric constraints $\boldsymbol{\phi}(\mathbf{q}) \in \mathbb{R}^m$. The matrix $\mathbf{H} \in \mathbb{R}^{n \times l}$ is the distribution matrix of the actuator forces/torques collected in the input vector $\mathbf{u} \in \mathbb{R}^l$. In addition $\mathbf{Q}_g(\mathbf{q})$ denotes the generalized force vector associated with gravity. It is assumed that the dimension of the control input l is less than the degrees of freedom $n - m$ of the mechanical system.

For the sake of simplicity, for the recent derivation we assume that the geometric constraints have no components with explicit time dependence. Then these constraints can be expressed at the acceleration level as

$$\ddot{\boldsymbol{\phi}} = \Phi_{\mathbf{q}}(\mathbf{q})\ddot{\mathbf{q}} + \dot{\Phi}_{\mathbf{q}}(\mathbf{q}, \dot{\mathbf{q}})\dot{\mathbf{q}}. \quad (3)$$

The servo constraint equations are formulated similar to the geometric constraint equations, but they involve control specification terms that may depend on time explicitly. These constraints are represented by

$$\boldsymbol{\phi}_s(\mathbf{q}, t) = \mathbf{0}, \quad (4)$$

which can also be defined at the acceleration level in the form

$$\begin{aligned} \ddot{\boldsymbol{\phi}}_s &= \mathbf{G}_{\mathbf{q}}(\mathbf{q})\ddot{\mathbf{q}} + \boldsymbol{\gamma}(\mathbf{q}, \dot{\mathbf{q}}, t) \quad \text{with} \\ \boldsymbol{\gamma}(\mathbf{q}, \dot{\mathbf{q}}, t) &= \dot{\mathbf{G}}_{\mathbf{q}}\dot{\mathbf{q}} + \frac{d}{dt} \frac{\partial \boldsymbol{\phi}_s}{\partial t}, \quad \mathbf{G}_{\mathbf{q}} = \frac{\partial \boldsymbol{\phi}_s}{\partial \mathbf{q}}. \end{aligned} \quad (5)$$

In addition, the equation of motion (1) can be projected into the nullspace of the actuator forces by applying the transformation $\mathbf{V} = \text{Null}(\mathbf{H}^T)^T$, which result in $n - l$ equations that describe the uncontrolled dynamics of system

$$\mathbf{V}(\mathbf{q})\mathbf{M}(\mathbf{q})\ddot{\mathbf{q}} + \mathbf{V}(\mathbf{q})\Phi_{\mathbf{q}}^T(\mathbf{q}) = \mathbf{V}(\mathbf{q})(\mathbf{Q}_g(\mathbf{q}) - \mathbf{c}(\mathbf{q}, \dot{\mathbf{q}})). \quad (6)$$

Combining the projected equation (6) with the constraint equations (3) and (5) the internal dynamics of the closed loop system is described by the $(n - l) + m + l = n + m$ equations

$$\begin{bmatrix} \mathbf{VM} & \mathbf{V}\Phi_{\mathbf{q}}^T \\ \Phi_{\mathbf{q}} & \mathbf{0} \\ \mathbf{G}_{\mathbf{q}} & \mathbf{0} \end{bmatrix} \begin{bmatrix} \ddot{\mathbf{q}} \\ \boldsymbol{\lambda} \end{bmatrix} = \begin{bmatrix} \mathbf{V}(\mathbf{Q}_g - \mathbf{c}) \\ -\dot{\Phi}_{\mathbf{q}}\dot{\mathbf{q}} \\ -\boldsymbol{\gamma} - \mathbf{K}_D\dot{\boldsymbol{\phi}}_s - \mathbf{K}_P\boldsymbol{\phi}_s \end{bmatrix}, \quad (7)$$

where $\boldsymbol{\lambda}$ is the vector of Lagrangian multipliers, while \mathbf{K}_P and \mathbf{K}_D are the proportional and derivative gain matrices. These gain

matrices have exactly the same role as the Baumgarte stabilization parameters during the solution of differential algebraic equations of motion. The PD control mechanism stabilizes the servo constraints and therefore it provides the desired motion of the system.

Then, assuming that the augmented mass matrix is invertible, equation (7) can be solved for the generalized accelerations $\ddot{\mathbf{q}}$ and for the Lagrangian multipliers $\boldsymbol{\lambda}$. The transformation \mathbf{H}^T projects equation (1) into the image of \mathbf{H} forming l independent equations for the control inputs in the form

$$\mathbf{u} = \mathbf{H}^\dagger (\mathbf{M}\ddot{\mathbf{q}} + \mathbf{c} + \Phi_q^T \boldsymbol{\lambda} - \mathbf{Q}_g) \quad (8)$$

where $\mathbf{H}^\dagger = (\mathbf{H}^T \mathbf{H})^{-1} \mathbf{H}^T$ is the generalized inverse of the actuator force/torque distribution matrix \mathbf{H} .

EXPERIMENTAL SETUP AND MECHANICAL MODEL

The validating experiments of the proposed control algorithm were carried out by using the Quanser 2DoF haptic device shown in Figure 1. This robot has two special cable driven actuators that drive the joints which have a common fixed rotation axis. The centers of masses of the driven (proximal) links are close to this axis, while the distal links have low inertia.

In order to use the device as an underactuated robot one of the actuators must be switched off, but the corresponding encoder signal is still necessary to determine the position of the end-effector. For this reason, it is not possible to dismount the unused actuator. In addition, it has to be noted that due to the gear ratio ($K_g = 19.3$) of the special cable actuated system the effective dry friction at the driven joints is significant. This fact, considering also the relatively low inertial coupling between the links, may prevent the motion of the link with the inactive motor.

To overcome this problem, a partial friction compensation was applied for the joint corresponding to the uncontrolled actuator. In addition, the weak inertial coupling between the links was strengthened by connecting the proximal links of the device through a virtual spring as shown in Figure 2. The realization of these solutions, however, requires the use of both actuators. Utilizing that the robot is a haptic device both actuators were used for the realistic rendering of the combined physical-virtual system, while the desired computed torque was superimposed to the torque output of one of these actuators only.

The mechanical model and the joint angles used for the kinematic description of the 2DoF pantograph are shown in Figure 2. Each link is modeled as a planar rigid body and the points CM_i , $i = 1 \dots 4$ in Figure 2 denote the centers of masses of the corresponding links. The locations of these points are defined by the local (or body frame) coordinates ξ_{CM_i} and η_{CM_i} . The origin of the local frames are attached to the input joints of the links such that coordinate ξ points toward the output joint and axis η

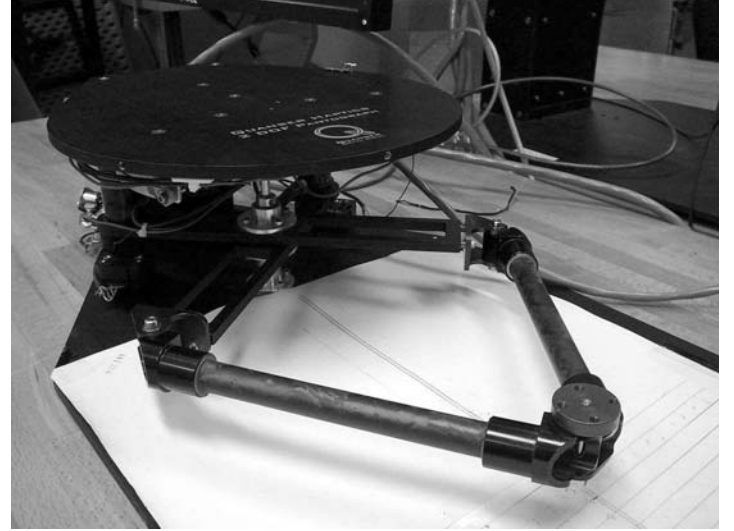


FIGURE 1. QUANSER 2DOF PANTOGRAPH

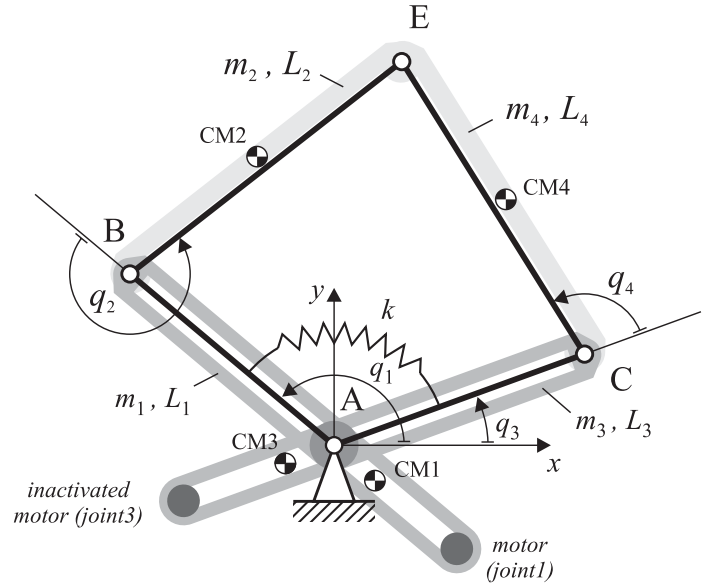


FIGURE 2. MECHANICAL MODEL

is implicitly defined by aligning the local ζ axis with the z axis of the fixed frame $\{x, y, z; A\}$.

The mechanical parameters were identified by a series of experiments and they are collected in Table 1. These parameters also include the lengths, masses and mass moment of inertia parameters of the links that are obtained from the CAD model of the device. The main sources of the viscous damping and dry friction are the electrical motors and the special cable based actuation mechanism. These parameters were also measured and tuned based on comparison of simulation and experimental results.

TABLE 1. MECHANICAL PARAMETERS

Description	Parameter	Value
Mass of Link_1	m_1	0.2820 kg
Mass of Link_2	m_2	0.0543 kg
Mass of Link_3	m_3	0.2820 kg
Mass of Link_4	m_4	0.0543 kg
Length of Link_1	L_1	0.147 m
Length of Link_2	L_2	0.199 m
Length of Link_3	L_3	0.147 m
Length of Link_4	L_4	0.199 m
CM location of Link_1	ξ_{CM1}	-0.0456 m
	η_{CM1}	0.0001 m
CM location of Link_2	ξ_{CM2}	0.0902 m
	η_{CM2}	0.0075 m
CM location of Link_3	ξ_{CM3}	-0.0456 m
	η_{CM3}	-0.0001 m
CM location of Link_4	ξ_{CM4}	0.0902 m
	η_{CM4}	-0.0075 m
Inertia of Link_1 wrt. Joint_1	I_1	$3 \cdot 10^{-3}$ kgm ²
Inertia of Link_2 wrt. CM2	I_{CM2}	$0.341 \cdot 10^{-3}$ kgm ²
Inertia of Link_3 wrt. Joint_3	I_3	$3 \cdot 10^{-3}$ kgm ²
Inertia of Link_4 wrt. CM4	I_{CM4}	$0.341 \cdot 10^{-3}$ kgm ²
Damping at Joint_1	d_1	0.0045 Nms
Damping at Joint_3	d_3	0.0045 Nms
Friction torque at Joint_1	τ_{f1}	0.025 Nm
Friction torque at Joint_3	τ_{f3}	0.025 Nm

The equation of motion of the model presented in Figure 2 can be composed of the equations of motion of two planar elbow manipulators the free ends of which are constrained to move together by forming the tip of the depicted five-bar mechanism.

Thus, choosing the non-minimum set of generalized coordinates $\mathbf{q} = [q_1 \ q_2 \ q_3 \ q_4]^T$ and using the notations $\cos(q_i) = c_i$ and $\sin(q_i) = s_i$, $i = 1 \dots 4$, the mass matrix in (1) can be written in the block diagonal form $\mathbf{M}(\mathbf{q}) = \text{diag}(\mathbf{M}_1, \mathbf{M}_2)$ with

$$\mathbf{M}_1 = \begin{bmatrix} I_1 + I_{CM2} + & I_{CM2} + \\ m_2(L_1^2 + \xi_{CM2}^2 + \eta_{CM2}^2) + & m_2(\xi_{CM2}^2 + \eta_{CM2}^2) + \\ 2L_1m_2(c_2\xi_{CM2} - s_2\eta_{CM2}) & L_1m_2(c_2\xi_{CM2} - s_2\eta_{CM2}) \end{bmatrix}, \quad (9)$$

$$\mathbf{M}_2 = \begin{bmatrix} I_3 + I_{CM4} + & I_{CM4} + \\ m_4(L_3^2 + \xi_{CM4}^2 + \eta_{CM4}^2) + & m_4(\xi_{CM4}^2 + \eta_{CM4}^2) + \\ 2L_3m_4(c_4\xi_{CM4} - s_4\eta_{CM4}) & L_3m_4(c_4\xi_{CM4} - s_4\eta_{CM4}) \end{bmatrix}. \quad (10)$$

The generalized force vector $\mathbf{c}(\mathbf{q}, \dot{\mathbf{q}})$, which includes the centrifugal, Coriolis and damping terms as well as the generalized forces associated with the idealized virtual spring, becomes

$$\mathbf{c} = \begin{bmatrix} -L_1m_2(\eta_{CM2}c_2 + \xi_{CM2}s_2)(\dot{q}_2^2 + 2\dot{q}_1\dot{q}_2) \\ L_1m_2(\eta_{CM2}c_2 + \xi_{CM2}s_2)\dot{q}_1^2 \\ -L_3m_4(\eta_{CM4}c_4 + \xi_{CM4}s_4)(\dot{q}_4^2 + 2\dot{q}_3\dot{q}_4) \\ -L_3m_4(\eta_{CM4}c_4 + \xi_{CM4}s_4)\dot{q}_3^2 \end{bmatrix} + \begin{bmatrix} d_1\dot{q}_1 \\ 0 \\ d_3\dot{q}_3 \\ 0 \end{bmatrix} + \begin{bmatrix} \tau_{f1}\text{sgn}(q_1) \\ 0 \\ \tau_{f3}\text{sgn}(q_3) \\ 0 \end{bmatrix} + \begin{bmatrix} k(q_1 - q_3 - q_{10} + q_{30}) \\ 0 \\ -k(q_1 - q_3 - q_{10} + q_{30}) \\ 0 \end{bmatrix} \quad (11)$$

where q_{10} and q_{30} refer to the initial values of the corresponding coordinates. The damping coefficients d_1 , d_3 and the magnitudes τ_{f1} and τ_{f3} of the dry friction torques at the joints 1 and 3 are given in Table 1.

The constraint equation (2) can easily be determined by equating the x_E and y_E coordinates of the originally free ends of the two planar elbow manipulators

$$\phi = \begin{bmatrix} L_1c_1 + L_2c_2 - L_3c_3 - L_4c_4 \\ L_1s_1 + L_2s_2 - L_3s_3 - L_4s_4 \end{bmatrix}. \quad (12)$$

The corresponding constraint Jacobian is

$$\Phi_{\mathbf{q}} = \begin{bmatrix} -L_1s_1 & -L_2s_2 & L_3s_3 & L_4s_4 \\ L_1c_1 & L_2c_2 & -L_3c_3 & -L_4c_4 \end{bmatrix}. \quad (13)$$

Due to the selection of the relative joint coordinates as generalized coordinates the distribution matrix of the input torques $\mathbf{u} = [\tau_1 \ \tau_3]^T$ has the simple form

$$\mathbf{H} = \begin{bmatrix} 1 & 0 \\ 0 & 0 \\ 0 & 1 \\ 0 & 0 \end{bmatrix}. \quad (14)$$

Once the control objective is defined through the servo constraint equations (4) the derived generalized forces and coefficient matrices can be used to calculate the desired actuator torques according to equation (8).

For the simulation of the controlled motion of the system we transform the dynamic model into the minimum form corresponding to the set of generalized coordinates $\mathbf{p} = [q_1 \ q_3]^T$. Using the assumption of scleronomic constraint, according to [7], this is possible by applying the transformation $\dot{\mathbf{q}} = \mathbf{B}(\mathbf{q})\dot{\mathbf{p}}$ which leads to the differential equation $\mathbf{B}^T\mathbf{M}\mathbf{B}\ddot{\mathbf{p}} + \mathbf{B}^T(\mathbf{M}\dot{\mathbf{B}}\dot{\mathbf{p}} + \mathbf{c}) = \mathbf{B}^T(\mathbf{Q}_g + \mathbf{H}(\mathbf{q})\mathbf{u})$.

SIMULATION AND EXPERIMENTAL RESULTS

During simulation and experiments the robot was commanded to move along a circle shown in Figure 3. For the sake of simplicity, a fixed circle with radius $R = 0.075$ m was considered having its center at $x_0 = 0$ m and $y_0 = 0.25$ m. The corresponding scalar servo constraint equation is

$$\phi_s = (x(\mathbf{q}) - x_0)^2 + (y(\mathbf{q}) - y_0)^2 - R^2 = 0 \quad (15)$$

where $x(\mathbf{q})$ and $y(\mathbf{q})$ are the task-space coordinates of the end effector.

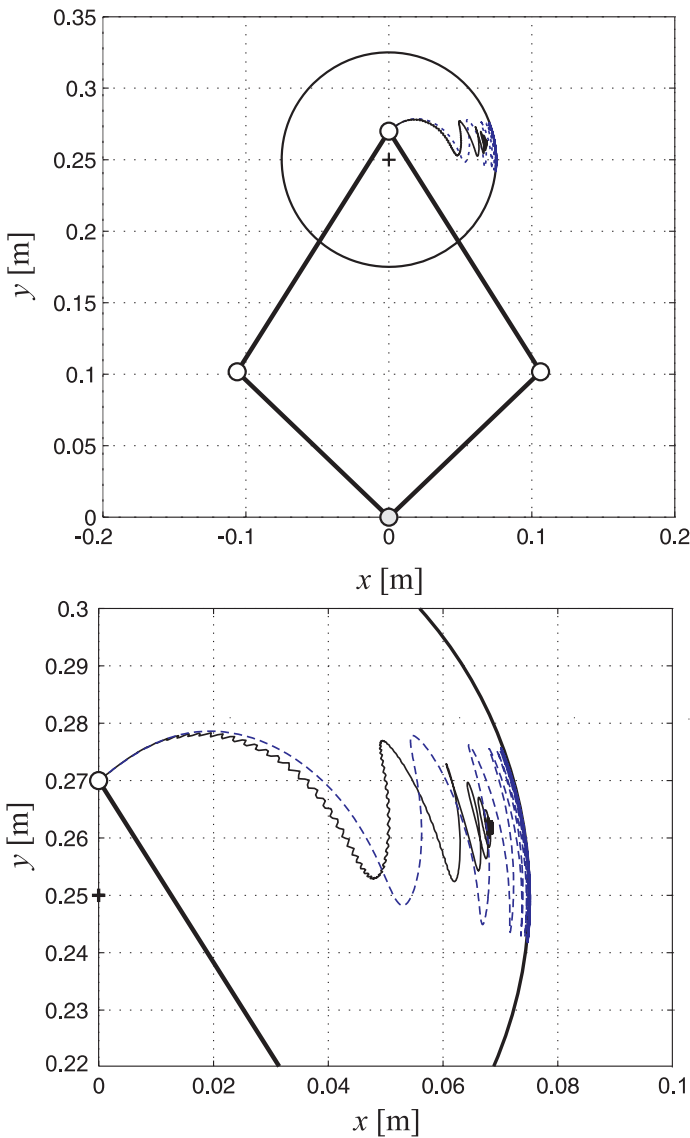


FIGURE 3. SIMULATION AND EXPERIMENTAL RESULTS

For the digital realization of the computed torque controller, the sampling time was selected to be 2 ms. This corresponds to the half of the maximum available sampling frequency of the hardware. The lower value was selected to obtain more reliable joint velocity data for the friction compensation during the experiments (without filtering). During the experiments, the viscous damping and the dry friction torques associated with joint 3 were partially eliminated via feedback compensation.

Another constraint on the experiments was the relatively low torque limit of the motor. The torque/current characteristic of the built in Maxon motors (118774) become nonlinear above the maximum continuous current limit which corresponds to the maximum joint torque $\tau_{max} = 0.6385$ Nm. Thus, in order to avoid nonlinear actuator force characteristics and saturation, the control gains were set to the relatively small values $K_P = 100$ and $K_D = 40$. These values and the selected virtual spring stiffness $k = 1$ N/m provided linear current-torque characteristics during the experiment.

The corresponding simulation results as well as the initial configuration of the robot are presented in Figures 3 and 4. In these figures the dashed blue lines correspond to the simulation results and the solid black lines represent the experimental results. Despite of the applied friction and damping compensation it can be seen that the experimental results are affected by considerable damping and due to the limited value of the proportional gain the steady state position error is relatively high. Using equation (4) the signed Euclidean error can be calculated as $R - \sqrt{\phi_s + R^2} = -5.4$ mm. Apart from this fact, the results show a good qualitative agreement and the simulation results confirm the applicability of the proposed computed torque controller.

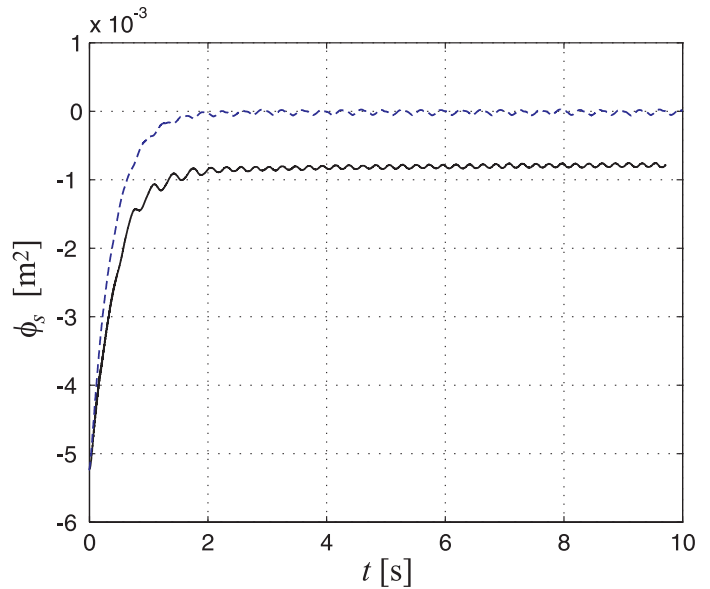


FIGURE 4. SERVO-COSNTRAIANT VIOLATION

CONCLUSIONS

In this paper a generalization of the computed torque control was presented for underactuated mechanical systems modeled by a non-minimum set of generalized coordinates. The proposed method relies on a formulation that can directly be applied to the arising set of DAE equations of motions. The applicability of the method was investigated by means of numerical simulation. The obtained results were verified by experiments conducted on the Quanser 2DoF pantograph. This haptic device has different performance and dynamics characteristics than ordinary underactuated robotic systems, but its haptic rendering capability made it possible to augment the physical system with a virtual spring component to realize stronger coupling between the elements of the device. The experimental results obtained by using the combined physical-virtual system and the corresponding simulation results show a good qualitative agreement.

ACKNOWLEDGMENT

This work was supported by the Hungarian National Science Foundation (OTKA K068910), the HAS-BME Research Group on Dynamics of Machines and Vehicles, the Canadian Foundation for Innovation, the Natural Sciences and Engineering Research Council of Canada (NSERC), and the Le Fonds Quebecois de La Recherche sur La Nature et Les Technologies (FQRNT). The support is gratefully acknowledged.

REFERENCES

- [1] Slotine, J., and Li, W., 1991. *Applied nonlinear control*. Prentice Hall.
- [2] Spong, M. W., 1994. "Partial feedback linearization of underactuated mechanical systems". In Proceedings of the IEEE International Conference on Intelligent Robots and Systems), Vol. 1, pp. 314–321.
- [3] Lammerts, I. M. M., 1993. "Adaptive computed reference computed torque control". PhD thesis, Eindhoven University of Technology.
- [4] de Jalón, J. G., and Bayo, E., 1994. *Kinematic and dynamic simulation of multibody systems: the real-time challenge*. Springer-Verlag.
- [5] Blajer, W., and Kolodziejczyk, K., 2008. "Modeling of underactuated mechanical systems in partly specified motion". *Journal of Theoretical and Applied Mechanics*, **46**(2), pp. 383–394.
- [6] Kovács, L. L., Zelei, A., Bencsik, L., Turi, J., and Stépán, G., 2010. "Motion control of an under-actuated service robot using natural coordinates". In Proceedings of the ROMANSY 18 Robot Design, Dynamics and Control (RomanSy 2010)), pp. 331–338.
- [7] Kövecses, J., Piedoboeuf, J.-C., and Lange, C., 2003. "Dynamic modeling and simulation of constrained robotic systems". *IEEE/ASME Transactions on mechatronics*, **8**(2), pp. 165–177.